Electronic Supplementary Material (ESI) for Nanoscale.

Supplementary Information

Putting Together the Puzzle of Ion Transfer in Single-Digit Carbon Nanotubes: Mean-Field Meets Ab Initio

Vadim Neklyudov[†] and Viatcheslav Freger[*,†,‡,¶]

[†]*Wolfson Department of Chemical Engineering, Technion - IIT, Haifa 32000, Israel*

[‡]*Russel Berrie Nanotechnology Institute, Technion - IIT, Haifa 32000, Israel*

[¶]*Grand Technion Energy Program, Technion - IIT, Haifa 32000, Israel*

E-mail: vfreger@technion.ac.il

Phone: +972 (0) 4 829 2933

Computation of hydration and transfer energies

The cycles for computing the thermodynamics quantities for hydration of water and ionic species in water bulk, which is used for benchmarking the *ab initio* computations, and transfer of ions and ion pairs from water to CNTP are schematically presented in Figure S2. The excess quantities for hydration of a water molecule ($\Delta X_{aq}[\mathrm{H_2O}]$) and ions ($\Delta X_{eq}[\mathrm{Ion}]$) in aqueous bulk relative to vacuum, where X is either E (electronic energy), H, G^{ex}, or S^{ex}, were calculated from computed X of corresponding single species in vacuum and in water clusters as follows:

$$\Delta X_{aq}[\mathrm{H_2O}] = 1/n \cdot X[(\mathrm{H_2O})_n] \tag{1}$$

$$\Delta X_{aq}[\mathrm{Ion}] = X[\mathrm{Ion}(\mathrm{H_2O})_n] - X[\mathrm{Ion}] - n\Delta X_{aq}[\mathrm{H_2O}]. \quad (2)$$

The equations for calculating the transfer energies of individual ions and ion pairs from water to CNTP are presented in the main text (see eqs. 9 and 10).

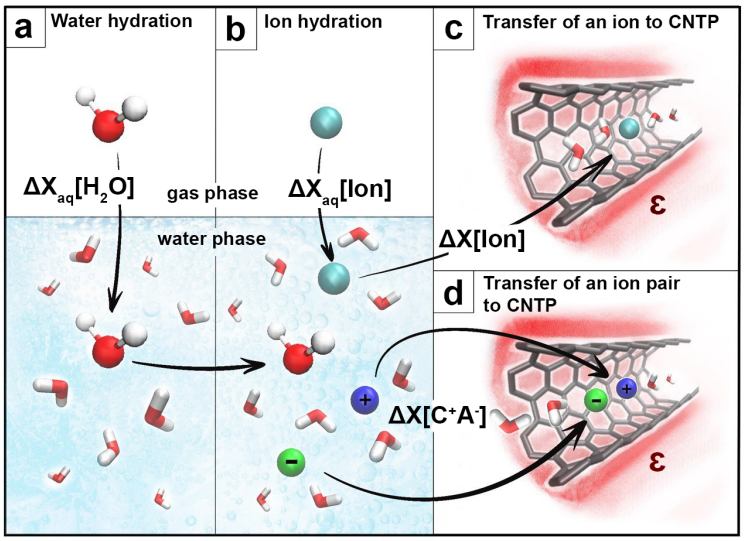

Figure S1: Thermodynamic cycles for computing energies of water hydration **(a)**, ion hydration **(b)** and transfer of an ion **(c)** or an ion pair **(d)** to CNTP. An ion and carbon, oxygen, and hydrogen atoms are cyan, grey, red, and white, respectively; positive and negative ions are presented as blue and green. Water clusters with and without an ion are embedded in a polarizable continuum with dielectric constant 78.36 representing bulk water. The CNTPs are surrounded by a continuum of dielectric constant ϵ.

Benchmarking of hydration energies and interaction with benzene

Figure S2a compares the computed thermodynamic quantities for hydration of water and ions with experimental values. It demonstrates that the selected level of theory (wB97XD/6-31G(d,p)) adequately reproduces the hydration thermodynamics. Figure S2b demonstrates a comparison of the experimental and calculated values of the enthalpies of interaction of water and potassium ion with benzene, as a surrogate model of the nanotube wall, showing a reasonable agreement a well.

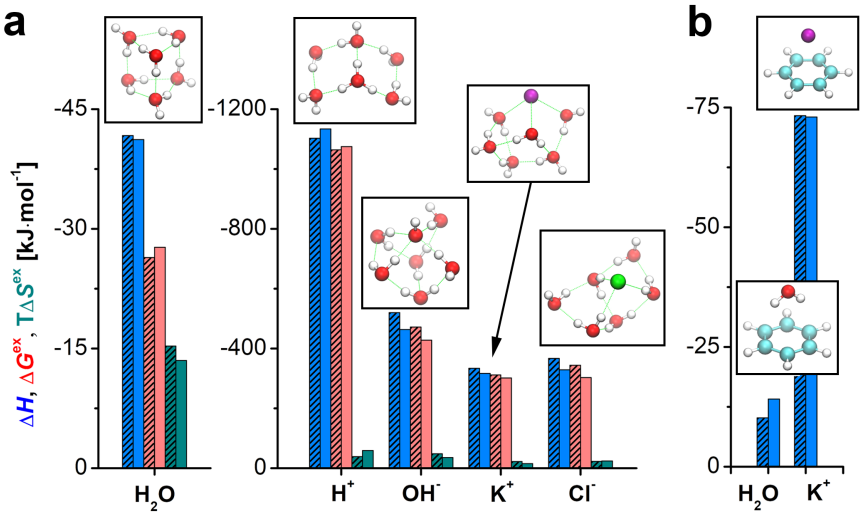

Figure S2: (A) The benchmarking of calculated hydration energies (non-shaded bars) of H_2O, H^+, OH^-, K^+ and Cl^- with them experimental values (shaded bars). Blue, red and dark green bars are entalpies, excess Gibbs energies and entropies, respectively. The optimized clusters embedded into IEFPCM model are also presented. **(B)** Experimental and calculated enthalpies of benzene complex with H_2O and K^+. All energies are obtained under standard conditions (298.15 K, 1 bar). The experimental values are from *Y. Marcus John Wiley & Sons, 2015* [1]

Derivation of the relation for CNTP conductance

The derivation is for the case when both ion uptake and conductance are controlled by free potassium and hydroxide ions, eq. 4 in the main text. Further, the assumption of a local mean-field electric potential is used, while this potential may vary along CNTP. The total steady-state current I flowing through the CNTP sums up the currents carried by each ion, which can be related to the gradients of the electric potential and ion concentrations using the following Nernst-Planck equation

$$\frac{I}{F} = \frac{I_K + I_{OH}}{F} = -\bar{D}_K \bar{C}_K (\nabla \ln C_K + \nabla\phi) + \bar{D}_{OH} \bar{C}_{OH} (\nabla \ln C_{OH} - \nabla\phi), \tag{3}$$

where I_i, $\bar{D}_i$ and $\bar{C}_i$ are, respectively, the current, diffusion (mobility) coefficient, and local concentration of species i within CNTP and the signs before different terms account for ion charges. The expressions in brackets are driving forces made up of chemical and electric potential gradients, where C_i (no bar) should be understood as respective equilibrium

concentrations in solution. To make the notation compact, here $\bar{C}_i$ are taken as linear concentrations obtained by multiplying volume concentrations in the channel by the channel cross-section area πr_c^2, where r_c is the channel radius, and potential ϕ is dimensionless, in units of thermal potential RT/F.

Local electroneutality within CNTP implies $\bar{C}_{OH} = \bar{C}_K = \alpha(C_K C_{OH})^{1/2}$, where $\alpha = \pi r_c^2 \exp\left(-\frac{\Delta G_K^{ex} + \Delta G_{OH}^{ex}}{2RT}\right)$ plays the role of the partitioning coefficient (cf. eq. 3 in the paper). The expressions for currents of individual ions I_K and I_{OH} may then be recast as follows

$$\frac{I_K}{\alpha F \bar{D}_K}(C_K C_{OH})^{-1/2} = -\nabla \ln C_K - \nabla\phi, \tag{4}$$

$$\frac{I_{OH}}{\alpha F \bar{D}_{OH}}(C_K C_{OH})^{-1/2} = +\nabla \ln C_{OH} - \nabla\phi. \tag{5}$$

After subtracting eq. 5 from eq. 4 and multiplying by $(C_K C_{OH})^{1/2}$, we obtain

$$\frac{1}{\alpha F}\left(\frac{I_K}{D_K} - \frac{I_{OH}}{D_{OH}}\right) = -(C_K C_{OH})^{1/2}\nabla \ln (C_K C_{OH}) = -2\nabla (C_K C_{OH})^{1/2} \tag{6}$$

Since all terms at the l.h.s. of eq. 6 are constant, it may be integrated to derive the linear variation of $(C_K C_{OH})^{1/2}$ along the CNTP (coordinate $0 \le x \le L$)

$$(C_K C_{OH})^{1/2} = (C_K C_{OH})_{x=0}^{1/2} - \frac{1}{2\alpha F}\left(\frac{I_K}{D_K} - \frac{I_{OH}}{D_{OH}}\right) x = (C_K C_{OH})_{x=0}^{1/2} + \frac{x}{L}\Delta (C_K C_{OH})^{1/2}, \tag{7}$$

which also indicates that the r.h.s. of eq. 6 is simply $-2\Delta(C_K C_{OH})^{1/2}/L$. (Here and below Δ designates the difference between the two solutions connected with CNTP.)

Conversely, after adding up eqs. 4 and 5 and integrating over the entire CNTP length, we obtain

$$\frac{1}{\alpha F}\left(\frac{I_K}{\bar{D}_K} + \frac{I_{OH}}{\bar{D}_{OH}}\right) = \frac{1}{\beta}\left[-2\Delta\phi - \Delta \ln C_K + \Delta \ln C_{OH}\right], \tag{8}$$

where $\beta = \int_0^L (C_{OH}C_K)^{-1/2} dx$. Equation 7 can be used to obtain β

$$\beta = \frac{L}{\Delta(C_{OH}C_K)^{1/2}} \int_0^L d\ln(C_{OH}C_K)^{1/2} = L\frac{\Delta \ln(C_{OH}C_K)^{1/2}}{\Delta(C_{OH}C_K)^{1/2}} = \frac{L}{\langle(C_{OH}C_K)^{1/2}\rangle_{l.m.}}. \quad (9)$$

Finally, we define ion transport numbers $t_K = \frac{\bar{D}_K}{\bar{D}_K+\bar{D}_{OH}}$ and $t_{OH} = \frac{\bar{D}_{OH}}{\bar{D}_K+\bar{D}_{OH}} = 1 - t_K$ and use the relation $I_{OH} = I - I_K$ to combine eqs 6, 8, and 9, find I_K and I_{OH} and obtain eq. 10

$$I = I_K + I_{OH} = G\left[-\Delta\phi - t_K\Delta \ln C_K + t_{OH}\Delta \ln C_{OH}\right], \quad (10)$$

where the expression in square brackets defines the total potential difference driving the current and the effective CNTP conductance is given by

$$G = \frac{\alpha F(\bar{D}_K + \bar{D}_{OH})}{\beta} = \frac{\alpha F(\bar{D}_K + \bar{D}_{OH})}{L}\langle(C_{OH}C_K)^{1/2}\rangle_{l.m.} \quad (11)$$

When the potential is expressed in Volts, eq. 11 should be multiplied by F/RT to obtain conductance in Siemens. It is easy to see that, when the product $C_{OH}C_K$ largely differs for the two solutions, the conductance is mainly controlled by the solution with the larger $C_{OH}C_K$.

Limiting rate of salt permeation

The limiting rates for permeation of the salt ions, K^+ and Cl^-, are calculated similar to eq. 11 for OH^- in the main text. Taking transport of Cl^- as an example and typical values of chloride mobility in water 2×10^{-9} m^2/s, van der Waals radius of (6,6) channel $r_c = 0.34$ nm and salt concentration $C_s = 0.1$ mol/L, the limiting molar rate, i.e., maximal rate of chloride diffusion towards or away from the CNTP mouth through the adjacent solution, is given by

$$Q = \frac{It_{Cl}}{F} = 2\pi C_{Cl,bulk} D_{Cl} r_c = 0.4 \cdot 10^{-16} \text{ mol/s}. \tag{12}$$

We see that this rate is of the order 10^{-16} mol/s, while experimentally observed rates at this salt concentration is of order 10^{-23} mol/s, cf. Fig. 2b in the main text. Similar result is easily obtained for other concentrations as well. The diffusion of the salt ions, chloride and potassium, through solution adjacent to the CNTP mouth is then not a limiting factor, i.e., this type of access resistance has significant effect on measured permeation rates.

Transfer parameters for ions and ion pairs obtained from *ab initio* calculations

Single ion trasfer

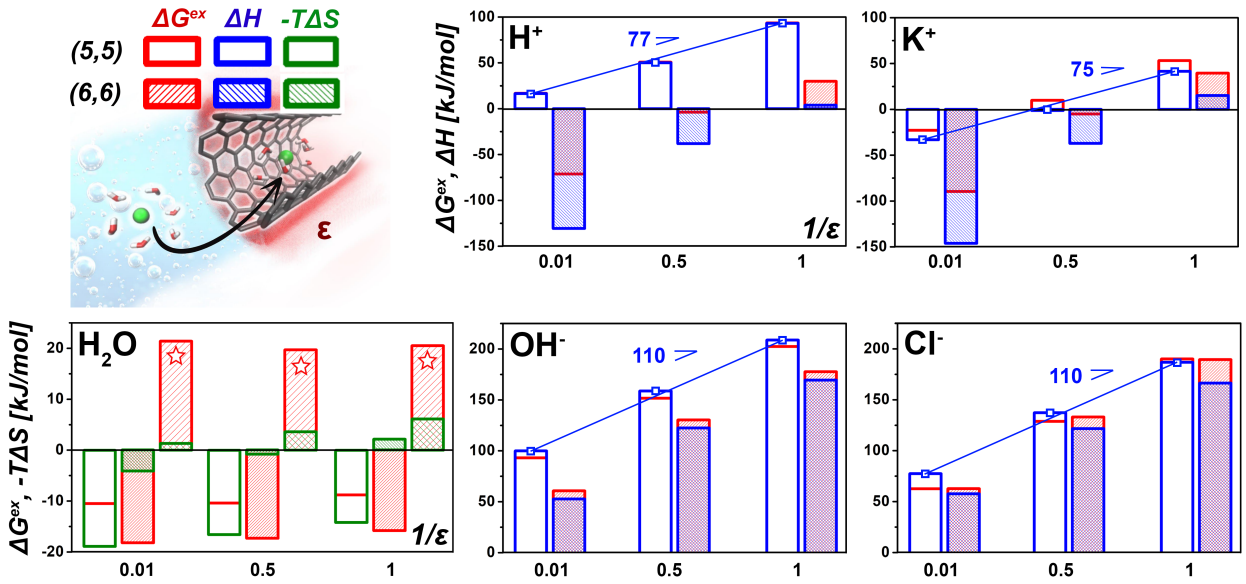

Figure S3: The transfer quantities for water and ions in (5,5) CNTP. For water transfer, the stars indicate triple-bonded water arrangement inside (6,6) CNTP. The slopes represent the dielectric energy.

Table S1 presents thermodynamics data for the transfer of single ionic species within CNT(6,6) and CNT(5,5). The results for CNT(6,6) include results the zigzag and triple-

bonded (3-bonded) arrangement of water. Fig. S3 presents the same data as bar diagrams to facilitate comparison with Fig. 1f in the main text.

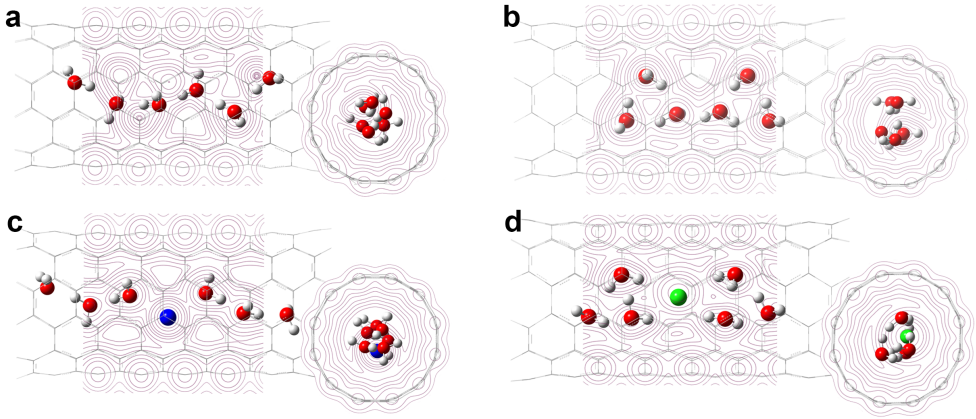

Figure S4: The maps of electron density distribution for single-file (**a**) and 3-bonded (**b**) water arrangements and for hydrated potassium (**c**) and chloride (**d**) ions in CNTP (6,6). In each case the cross-sections along and across main axis in the middle point are shown.

Transfer of contact and water-separated KOH pairs

Fig. 3a in the main text shows transfer energies for different contact pairs between relevant ions as a proxy of ion-ion interaction. However, such interactions are expected to weaken with the distance between the ions, eventually approaching the free-ion limit. To clarify this effect and quantify the attenuation of ion-ion interaction with distance, in addition to the thermodynamic transfer parameter of K^+OH^- ionic pair, they were compute for KOH pairs with ions separated by one and two water molecules, which is summarized in Table S2. It is seen that, as the separation between K^+ and OH^- increases, the transfer energy increases, i.e., transfer becomes less favorable, approaching that of separate free K^+ and OH^- ions (last line in Table S2). Specifically, the gain in enthalpy drops, changing sign for two-molecule separation, which is only partly compensated by decreasing entropic penalty.

Table S1: The transfer energies (ΔG^{ex}, ΔH, $-T\Delta S^{ex}$) of species under consideration at different dielectric constants outside CNT(6,6) and (5,5) (in parenthesis) calculated at wB97X-D/6-31G(d,p). From left to right: CNT(6,6) 3-bonded / CNT(6,6) zigzag / CNT(5,5)

Species	$\epsilon = 1$	$\epsilon = 2$	$\epsilon = 100$
Excess Gibbs transfer energies (ΔG^{ex})			
H_2O	20.5/-15.8/-8.8	19.7/-17.3/-10.4	21.4/-18.2/-10.5
H^+	40.0/29.9/93.5	7.4/-3.8/50.8	-33.7/-71.3/16.8
OH^-	177.7/167.6/202.4	130.3/119.0/151.6	60.7/23.1/93.0
K^+	49.6/39.5/53.2	6.1/-5.1/9.9	-52.0/-89.6/-22.8
Cl^-	189.5/179.4/190.1	133.1/121.8/128.7	62.7/25.1/62.6
Enthalpy of transfer (ΔH)			
H_2O	14.4/-17.9/5.4	16.0/-16.5/6.2	20.1/-14.1/8.4
H^+	32.3/3.8/93.1	-0.3/-38.1/50.0	-41.2/-130.7/16.5
OH^-	169.4/140.8/208.8	122.4/84.6/58.7	52.7/-36.8/99.9
K^+	43.5/15.0/41.4	0.7/-37.1/-1.2	-56.6/-146.2/-33.2
Cl^-	166.3/137.8/186.8	121.7/83.8/137.3	57.7/-31.9/77.5
Excess entropy of transfer (-TΔS^{ex})			
H_2O	6.1/2.1/-14.2	3.6/-0.8/-16.6	1.3/-4.1/-18.9
H^+	7.7/26.1/0.5	7.7/34.3/0.8	7.4/59.4/0.3
OH^-	8.4/26.8/-6.4	7.8/34.4/-7.1	7.9/59.8/-6.9
K^+	6.1/24.5/11.8	5.4/32.0/11.1	4.6/56.5/10.4
Cl^-	23.2/41.5/3.3	11.4/38.0/-8.5	5.0/56.9/-14.9

Ionic mobilities in CNTPs

The experimental and calculated values of the diffusion coefficients of ions and water compiled from literature are summarized in Table S3. In general, the calculated and experimental values of the diffusion coefficients of water in CNT(6,6) are within reasonably low range, except for one outstanding results water in (6,6) tubes at pH 3. The values of the diffusion coefficients of water and K^+ and Li^+ ions, computed and obtained using by NMR for Li^+ in wider 1.5 nm CNTPs, are close both to each other and to the respective diffusivities in bulk water, D_K 1.96 $\times$ 10^{-5} cm^2/s, D_{Li} 1.03 $\times$ 10^{-5} cm^2/s.[9] Thus, for calculations requiring the diffusion coefficients of ions and water, we approximated them for bulk values. However, the diffusivities of H^+ and OH^- ions are known to be larger due to Grotthus mechanism. In CNTP(6,6), computations agree well and indicate they are larger than water bulk values

Table S2: Thermodynamics of water separated and contact K^+OH^- ionic pairs from water bulk to CNT(6,6) at $\epsilon = 2$

Ionic pair	ΔG, kJ/mol	ΔH, kJ/mol	-TΔS, kJ/mol
K^+OH^-	-61.6	-87.5	25.9
$K^+/H_2O/OH^-$	-16.8	-24.1	7.3
$K^+/2H_2O/OH^-$	7.2	4.6	2.6
Free K^+ and OH^-	62.6	42.5	20.1

Table S3: Summarized experimental and calculated mobilities of water and ions

Species	D, cm^2/s	Conditions	Ref.
H_2O	$4.4 \pm 0.2 \cdot 10^{-5}$ (exp.)	CNT(6,6) pH 3.0	[2]
	$8.9 \pm 0.4 \cdot 10^{-6}$ (exp.)	CNT(6,6) pH 7.8	[2]
	$1.13 \cdot 10^{-4}$ (calc.)	CNT(6,6) pH 3.0	[2]
	$1.07 \cdot 10^{-5}$ (calc.)	CNT(6,6)	[3]
	$1.2 \cdot 10^{-5}$ (calc.)	CNT(7,7)	[4]
	$2.2 \cdot 10^{-5}$ (exp.)	1.5 nm CNTP	[5]
	$2.3 \cdot 10^{-5}$ (calc.)	1.5 nm CNTP	[5]
	$1.5 \cdot 10^{-5}$ (calc.)	CNT(7,7)	[6]
K^+	$1.9 \cdot 10^{-5}$ (calc.)	1.5 nm CNTP	[5]
Li^+	$1.2 \cdot 10^{-5}$ (exp.)	1.5 nm CNTP	[5]
	$1.1 \cdot 10^{-5}$ (calc.)	1.5 nm CNTP	[5]
H^+	$17 \cdot 10^{-4}$ (calc.)	CNT(6,6)	[7]
	$19.3 - 32.1 \cdot 10^{-4}$ (calc.)	CNT(6,6)	[8]
OH^-	$24.1 - 32.2 \cdot 10^{-4}$ (calc.)	CNT(6,6)	[8]

(D_{H+} 9.31 $\times$ 10^{-5} cm^2/s, D_{OH-} 5.27 $\times$ 10^{-5} cm^2/s[9]) and similar for both ions. The value of OH^- diffusivity used in model fitting (see next), 24 $\times$ 10^{-4} cm^2/s, was then selected based in the values computed for CNTP (6,6).

Fitting of transfer excess Gibbs energies to experimental data on conductivity and anion permeation in vesicles

For pH 7.5, i.e., $C_{OH} = 10^{-6.5}$ M, the conductivity shows a linear dependence on $(C_s C_{OH})^{1/2}$. These data presented in Figure 2a were fitted to the above equation for conductivity for pH

7.5, eq. 13, which was recast in the following form

$$G(\text{pH } 7.5) = \frac{F^2}{RT}\frac{\pi r_c^2}{L}(\bar{D}_K + \bar{D}_{OH})(C_{OH}C_K)^{1/2}\exp\left(-\frac{\Delta G_h^{ex}}{RT}\right) \tag{13}$$

The diffusion coefficients of K^+ and OH^- were approximated as explained in the last section. Using $L = 10.6$ nm and van der Waals radius of CNTP(6,6) $r_c = 0.34$ nm, G_h^{ex} was viewed as the only adjustable parameter, computed from the slope of the fitted linear dependence passing through the origin (zero intercept) to obtain $G_h^{ex} = -3.1 \pm 0.8$ kJ/mol.

The analogous relation for pH 3, linear in C_s, is

$$G(\text{pH } 3) = \frac{F^2}{RT}\frac{\pi r_c^2}{L}(\bar{D}_K + \bar{D}_{Cl})C_s\exp\left(-\frac{\Delta G_s^{ex}}{RT}\right) \tag{14}$$

Using as estimates bulk values D_K 1.96×10^{-5} cm^2/s and D_{Cl} 2.03×10^{-5} cm^2/s (see last section), the slope fitted to linear dependence of G on C_s yield $G_s^{ex} = 7.6 \pm 0.3$ kJ/mol.

In a similar manner, we fitted to the experimental chloride permeation rate Q_{Cl} at pH 7 in Fig. 2b to the relation

$$Q_{Cl}(\text{pH } 7.5) = \frac{\pi r_c^2}{L}\bar{D}_{Cl}C_s^{3/2}C_{OH}^{-1/2}\exp\left(-\frac{\Delta\tilde{G}_s^{ex}}{RT}\right), \tag{15}$$

The chloride transfer rate per CNTP in Fig. 2b was computed from the digitised row data for chloride flux in vesicles reported by Li et al.[10] and rescaled using the factor based on the chloride permeability reported in this paper. The the best fit to eq. 15 yielded the value $\Delta\tilde{G}_s^{ex} = 63.3 \pm 0.2$ kJ/mol presented in Fig. 2b.

Figure S5 also presents raw data form Li et al. scaled in 3 different ways. This demonstrates that, while the plot of chloride flux versus $C_s^{3/2}$ shows a good linear relation with zero intercept (panel b), the plots versus C_s and C_s^2 show a non-linear dependence, with a non-zero-intercept for linear fits.

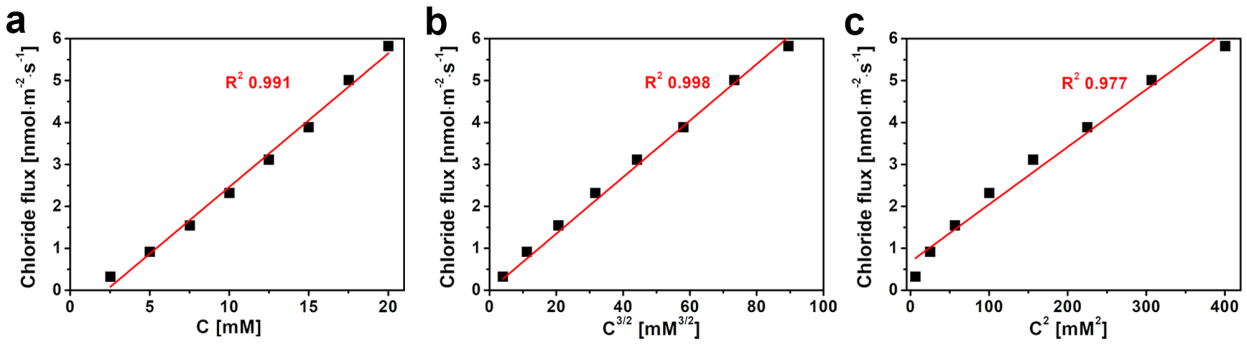

Figure S5: Chloride flux as a function of salt concentration. The data points were digitized from Li et al.[10]

Interpolation of the water transfer energies

For simplicity we consider the system has a very low compressibility and ignore the negligble differences between the Gibbs and Helmholtz free energies, G and F, as well as between internal energy and enthalpy, U and H. We then can use more common partition functions Q to express statistical thermodynamic relations for constant volume instead of its more complicated analogues for constant pressure. Thus F, U, Q are related as follows

$$e^{-F/RT} = Q = \sum \omega_i e^{-U_i/RT}, \tag{16}$$

$$U = \sum \omega_i U_i e^{-U_i/RT}/Q \quad \text{or} \quad \sum \omega_i U_i e^{-U_i/RT} = U e^{-F/RT} \tag{17}$$

where ω_i and U_i are the degeneracy and and energy of a state, respectively, and summation is over different states. We assume that zigzag and triple-bonded arrangements form two distinct minima, "1" and "2", in the energy landscape, around which most water molecules are found. When the transition between arrangements is unlikely due to a high barrier, the sums in above equations may be approximated by splitting to two subsums, whose values may be related to thermodynamic parameters, F_1, U_1 and F_2, U_2 computed by Gaussian for the situations, where the system is trapped in the corresponding arrangement as a local energy minimum. We may then approximately view the equilibrium as a superposition of the arrangements "1" and "2" weight by corresponding fractions x_1 and $x_2 = 1 - x_1$. We

then approximate F and U of the system as

$$e^{-F/RT} = x_1 e^{-F_1/RT} + (1-x_1)e^{-F_2/RT} \quad \text{and} \quad Ue^{-F/RT} = x_1 U_1 e^{-F_1/RT} + (1-x_1)U_2 e^{-F_2/RT} \tag{18}$$

The fraction x_1 of molecules that assume arrangement "1" is computed by requiring that the system is in equilibrium with bulk water, i.e., by setting total F equal to that of bulk water. We then may write down for corresponding transfer quantities (Δ designating difference between water in CNTP and bulk water)

$$e^{-\Delta F/RT} = x_1 e^{-\Delta F_1/RT} + (1-x_1)e^{-\Delta F_2/RT} = 1, \tag{19}$$

which gives x_1 as

$$x_1 = \frac{1 - e^{-\Delta F_2/RT}}{e^{-\Delta F_1/RT} - e^{-\Delta F_2/RT}} \approx e^{\Delta F_1/RT} \tag{20}$$

The last approximate relation holds, when $\Delta F_1/RT$ is large and negative and also much lower than $\Delta F_2/RT$ that is large and positive, as was obtained for the zigzag and triple-bonded states, respectively (cf. Fig. 1f in the main text). Note one of the arrangements "1" ad "2" must have a positive and the other a negative ΔF to allow equilibrium with water. Note that x_1 is then very small, i.e., only a small fraction of water will assume this arrangement, however, it will determine the transfer enthalpy. Indeed, using this x_1 and eq. 18, we find U as

$$U = x_1 U_1 e^{-\Delta F_1/RT} + (1-x_1)U_2 e^{-\Delta F_2/RT}) \approx U_1 + U_2(1 - e^{\Delta F_1/RT})e^{-\Delta F_2/RT} \approx U_1 \tag{21}$$

This also means $\Delta U \approx \Delta U_1$. Due to negligible difference between U and H, this also means $\Delta H \approx \Delta H_1$, i..e, transfer enthalpy will be dictated by the lowest free energy arrangement.

References

(1) Marcus, Y. *Ions in Solution and their Solvation*; John Wiley & Sons, 2015.

(2) Tunuguntla, R. H.; Henley, R. Y.; Yao, Y.-C.; Pham, T. A.; Wanunu, M.; Noy, A. Enhanced water permeability and tunable ion selectivity in subnanometer carbon nanotube porins. *Science* **2017**, *357*, 792–796.

(3) Binesh, A. R.; Kamali, R. Effects of chirality on single-file water permeability and diffusivity through single wall carbon nanotubes. *Micro & Nano Lett.* **2017**, *12*, 109–112.

(4) Barati Farimani, A.; Aluru, N. R. Spatial diffusion of water in carbon nanotubes: from fickian to ballistic motion. *J. Phys. Chem. B* **2011**, *115*, 12145–12149.

(5) Buchsbaum, S. F.; Jue, M. L.; Sawvel, A. M.; Chen, C.; Meshot, E. R.; Park, S. J.; Wood, M.; Wu, K. J.; Bilodeau, C. L.; Aydin, F., et al. Fast Permeation of Small Ions in Carbon Nanotubes. *Adv. Sci.* **2021**, *8*, 2001802.

(6) de Freitas, D. N.; Mendonça, B. H.; Köhler, M. H.; Barbosa, M. C.; Matos, M. J.; Batista, R. J.; de Oliveira, A. B. Water diffusion in carbon nanotubes under directional electric frields: Coupling between mobility and hydrogen bonding. *Chem. Phys.* **2020**, *537*, 110849.

(7) Dellago, C.; Naor, M. M.; Hummer, G. Proton transport through water-filled carbon nanotubes. *Phys. Rev. Lett.* **2003**, *90*, 105902.

(8) Lee, S. H.; Rasaiah, J. C. Proton transfer and the diffusion of H+ and OH- ions along water wires. *J. Chem. Phys.* **2013**, *139*, 124507.

(9) Haynes, W. M. *CRC handbook of chemistry and physics*; CRC press, 2014.

(10) Li, Y.; Li, Z.; Aydin, F.; Quan, J.; Chen, X.; Yao, Y.-C.; Zhan, C.; Chen, Y.; Pham, T. A.; Noy, A. Water-ion permselectivity of narrow-diameter carbon nanotubes. *Sci. Adv.* **2020**, *6*, eaba9966.